Reduction of NO_2 on Ceria Surfaces

Michael Nolan,[†,§] Stephen C. Parker,[‡] and Graeme W. Watson*[,†]

School of Chemistry, University of Dublin, Trinity College, Dublin 2, Ireland, and Department of Chemistry, University of Bath, Claverton Down, Bath, BA2 7AY, U.K.

Received: October 3, 2005

Cerium dioxide, CeO_2, plays an important role in catalysis, due to its ability to store and release oxygen depending on the conditions present in the catalyst environment. To understand the role of ceria in catalytic reactions, we need to study the details of the interaction of ceria surfaces with environmentally sensitive molecules. In this work, we examine the adsorption of the NO_2 molecule onto defective (reduced) surfaces of ceria using density functional theory with a correction for on-site Coulomb interactions (DFT+U), which allows for a consistent description of pure and reduced ceria. The interaction of NO_2 with defective (111), (110), and (100) surfaces gives an adsorbate−surface structure in which the bond lengths around one Ce(III) ion from the reduced surface shorten, while one N−O bond lengthens. Analysis of the electronic structure and spin density distributions demonstrates that one Ce(III) has been reoxidized to Ce(IV), with the formation of adsorbed NO_2^-. Finally, we discuss the energetics of the interaction of NO_2 with ceria.

1. Introduction

In the application of ceria in catalysis,[1] it has traditionally played the role of a support material, e.g., catalytic oxidation of CO on Pt[2] and reduction of NO on Rh[3] are both enhanced by using a ceria support material. However, with its ability to release and take up oxygen (the oxygen storage capacity, OSC), it has been demonstrated that ceria does not merely function as an inactive support. The oxidation of CO and reduction of NO_2 can be catalyzed with ceria, without need for use of precious metals.[4] In identifying the role of ceria within the catalyst, it is important to study the reactivity and chemisorptive properties of this material, through investigation of the interactions between molecules such as NO_2 and CO with ceria surfaces.

Oxygen vacancies in ceria are formed in the oxidation of CO to CO_2, where the surface gives up one oxygen atom and two neighboring Ce(IV) atoms are reduced to Ce(III), in Kroger−Vink notation

$$O^x_o + 2Ce^x_{Ce} \rightarrow V^{\cdot\cdot}_o + 2Ce'_{Ce} + {}^1/_2O_2$$

These vacancies are reactive sites and can interact with NO_2 to give NO, while the liberated oxygen atom participates in surface reoxidation, providing an initial step in the ultimate reduction of NO_2 to N_2.

Given the importance of the OSC of ceria, it is vital to have a comprehensive understanding of this material and subsequent interaction of pure and reduced surfaces with environmentally sensitive molecules. There are a number of recent experimental studies of the ceria−NO_2 interaction. Rodriguez et al.[4] studied NO_2 adsorption onto the (111) ceria surface, and Berner et al.[2] studied the interaction of NO_2 with the (111) surface of ceria on a Pt support. Namai et al.[5] used AFM to study the interaction of NO_2 with a slightly reduced CeO_2 (111) surface. Upon exposure of a stoichiometric (111) surface to NO_2, UV photoemission spectroscopy (UPS) showed no evidence of NO_2 dissociation,[4] while in AFM images, no change in surface structure was observed[5] indicating that NO_2 does not interact with an oxidized surface. On reduced ceria, however, NO_2 was found to dissociate into NO, coupled to a reduction in the intensity of the reduced Ce(III) peak in the UPS spectrum.[2,4] In AFM it was observed that exposure to NO_2 healed the oxygen vacancies previously present in the sample.[5] These results demonstrate the necessity for the presence of reduced Ce(III) ions in the surface, which promote the breaking of one NO bond so that NO_2 dissociates into NO and O, with the latter leading to oxidation of the surface. In these experiments no vibrational data was presented.

A number of first-principles studies of ceria have considered stoichiometric bulk[6,7] and surfaces.[8−10] Skorodumova et al. have also studied fully reduced bulk ceria (Ce_2O_3),[7] and Fabris et al. have studied formation of oxygen vacancies in the bulk (CeO_{2-x}).[11] Interatomic potential studies have been published in which the energetics of oxygen vacancy formation in ceria surfaces were considered.[12,13]

In recent studies, oxygen vacancies at the (111), (110), and (100) surfaces of ceria have been studied using first-principles density functional theory, DFT.[10,14,15] These studies have demonstrated that DFT cannot treat the electronic structure of oxygen vacancy defects in ceria surfaces. This is due to the incorrect DFT description of the highly localized Ce 4f states of Ce(III) ions that result from the formation of oxygen vacancies[10,14] and which have been observed in UPS experiments.[16] A consistent description of these localized, partially occupied states requires an approach beyond DFT, such as the DFT+U methodology[17,18] used in our work.[10,15] The DFT+U formalism can describe the highly localized Ce f-electronic states and provides a more consistent approach compared to that chosen by Skorodumova et al. in which they treated the Ce 4f electrons as core electrons[7] when studying reduced ceria. The latter is unsatisfactory, as it requires the Ce(III) ions to be selected in advance and thus cannot lead to a consistent description of defective ceria surfaces. The DFT+U methodol-

* Corresponding author. E-mail: watsong@tcd.ie.
† University of Dublin.
‡ University of Bath.
§ Present address. Tyndall National Institute, Lee Maltings Prospect Row, Cork, Ireland.

10.1021/jp055624b CCC: $33.50
Published on Web 01/19/2006

ogy offers the possibility to describe both Ce(IV) (stoichiometric ceria) and Ce(III) (reduced ceria) oxidation states in a single consistent framework, the validity of which has been demonstrated for modeling localized electronic states of a range of oxides.[10,15,17−19]

While the reduction of NO and NO_2 to N_2 on reduced ceria surfaces, with surface reoxidation, is of significant interest, there exist to date no first-principles studies of the NO_2 interaction with reduced ceria surfaces. The present paper marks the first study of the processes influencing the interaction of NO_2 on reduced ceria surfaces, building upon our studies of defective ceria surfaces. We consider the adsorption of NO_2 onto the reduced (111), (110), and (100) surfaces of ceria, in which the defects are generated through loss of an oxygen ion from the surface. We demonstrate the effect of NO_2 adsorption on the atomic and electronic structure of the defective surfaces and the molecule and discuss the relevant energetics.

2. Methods

All calculations presented herein were carried out with the Vienna ab initio simulation program (VASP).[20] The valence electronic states are expanded in a basis of plane waves, while the strongly oscillating wave functions of the core electrons are represented using the projector augmented wave (PAW) approach,[21] which provides an all-electron calculation with a frozen core; for Ce we have a [Xe] core and for O and N we have a [He] core. The exchange-correlation functional is the generalized gradient approximation, GGA, of Perdew and Wang, PW91.[22] DFT+U is chosen as our computational approach, due to the inability of GGA-DFT to describe the Ce 4f electronic states which result from formation of oxygen vacancies in ceria. GGA-DFT fails, since it uses an approximate exchange-correlation functional, which means that cancellation with the Hartree interaction for a single electron is not guaranteed. This introduces an electron self-interaction error (SIE). The SIE penalizes localization of electrons in partially occupied electronic states and favors delocalization of electrons. The DFT+U formalism introduces an on-site Coulomb interaction in these states, characterized by the parameter U. The SIE is reduced, and localization of electrons is possible. The result of this is that a gap opens up between the fully occupied states and the remaining unoccupied states, with the U parameter controlling this energy gap. In a DFT+U calculation, we have to determine a value of U. The approach we take is an empirical definition of U, through varying the value of U until the best agreement with the (limited) experimental data for the defective surfaces is achieved ($U = 5$ eV).[10,15]

In calculations with 3-D periodic boundary conditions, a surface is represented by a thin slab, which is separated from its images in the direction perpendicular to the surface by a vacuum gap, in this case 15 Å. The slab thicknesses are as follows: (111) surface 10.5 Å (12 atomic layers), (110) surface 11.5 Å (7 atomic layers), and (100) surface 10.94 Å (9 atomic layers). For the (111) and (100) surfaces, we use a $p(2 \times 2)$ expansion of the surface unit cell and for the (110) surface we have a $p(2 \times 1)$ expansion with these expansions of the surface unit cell contributing to a reduction in the effect of periodic defect−defect interactions so that the vacancy−vacancy distances are 7.74 Å (111), 7.74 Å (110), and 7.65 Å (100). With strong localization of electronic defects, these defect−defect distances are sufficiently large to provide consistent results. The cutoff energy for the plane wave basis is 500 eV, and for sampling of the Brillouin zone we have used a $2 \times 2 \times 1$ Monkhorst Pack sampling grid so that sampling along the vector separating the slabs is neglected. Oxygen vacancies are generated on both sides of the slab for the defective surfaces so that no dipole moment is present across the slab. Similarly, NO_2 is adsorbed onto both sides of the slab. Calculations of molecular NO_2, NO_2^-, and NO are carried out in the same simulation cell as the surface−adsorbate calculation, using the same exchange-correlation functional and plane wave cutoff, with sampling at the Γ-point. The lowest energy spin state for the neutral molecules is the doublet state, while the anion is spin paired. Full geometry relaxation of all surface−adsorbate structures was carried out. All calculations are spin polarized with the spin degrees of freedom allowed to relax.

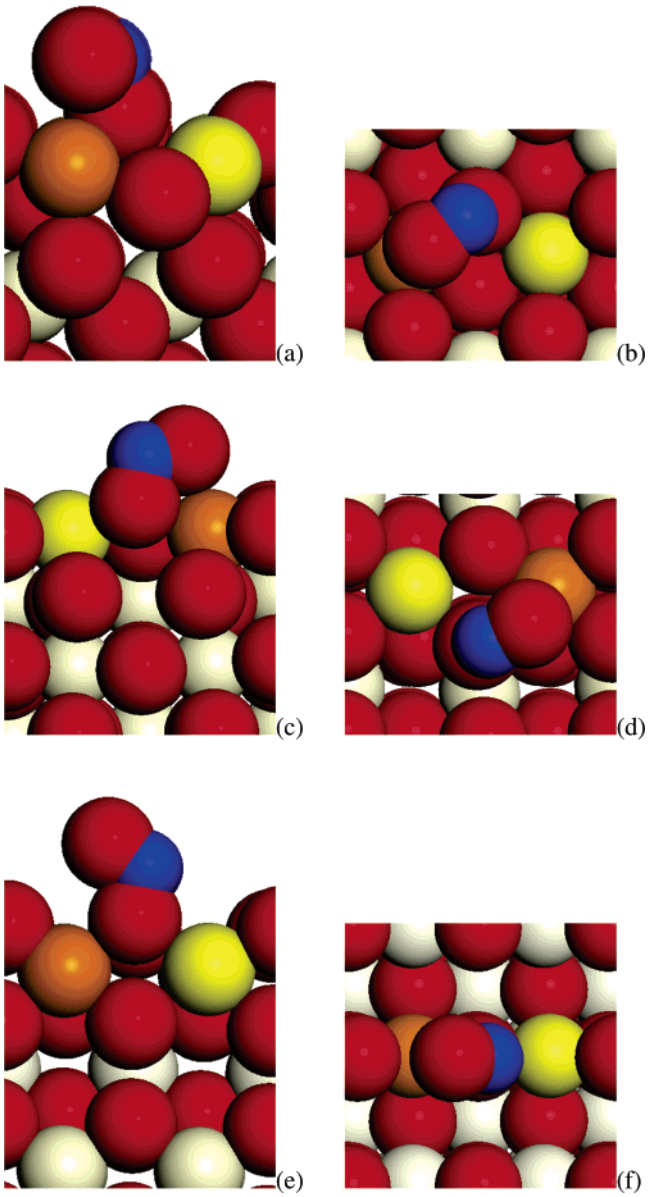

Figure 1. DFT+U geometry of NO_2 adsorbed on the defective ceria surfaces: (a, b) (111), (c, d) (110), (e, f) (100). The oxygen ions are red spheres, the Ce(IV) ions are smaller white spheres, the nitrogen is a blue sphere, the two Ce(III) ions of the reduced surfaces, Ce^A and Ce^B, are yellow and orange.

3. Results

3.1. Structure of Adsorbed NO_2 on Reduced Ceria Surfaces. The relaxed geometries of the surface−adsorbate structures for the three ceria surfaces are shown in Figure 1 a−f using space filling models. The oxygen ions are large red

TABLE 1: Ce(III)−O Distances (angstrom) for Stoichiometric and Reduced Ceria Surfaces and for Adsorbed NO_2 [a]

(111)

	stoichiometric	reduced	NO_2 adsorbed
Ce^A	3 × 2.36	2 × 2.37	2 × 2.42; O_V 2.80
Ce^B	3 × 2.36	2 × 2.37	2.30, 2.32; O_V 2.66

(110)

	stoichiometric	reduced	NO_2 adsorbed
Ce^A	4 × 2.33	2.27, 2.32, 2.40	2.35, 2.36, 2.43; O_V 2.77
Ce^B	4 × 2.33	2.27, 2.32, 2.40	2.19, 2.21, 2.24; O_V 2.60

(100)

	stoichiometric	reduced	NO_2 adsorbed
Ce^A	2 × 2.19	1 × 2.22	2.30; O_V 2.50
Ce^B	2 × 2.19	1 × 2.23	2.03; O_V 2.43

[a] The distances in column 1 are those to the nearest surface oxygen ions in the stoichiometric surfaces, while in column 2 we present the Ce(III)−O distances in the reduced surface, and the third column presents the Ce(III)−O distances upon NO_2 adsorption, while the distance in the third column marked with O_V is the distance to the O_V oxygen atom. The designation Ce^A, Ce^B is elaborated upon in the text.

spheres, nitrogen is the blue sphere, and the Ce(IV) ions are small white spheres. For ease of discussion, the two reduced Ce(III) ions of the initial defective surface are indicated by the yellow, "Ce^A", and the orange, "Ce^B", spheres in Figure 1; the use of this nomenclature will facilitate discussion of the change in the structure and electronic structure of the surface. Figure 1 shows that the NO_2 molecule adsorbs onto the surface through one of the oxygen atoms, which occupies the vacancy site. The molecule displays a bent configuration with the remaining N−O bond pointing toward Ce^B; we denote the oxygen atom of the NO_2 molecule that sits at the vacancy site by O_V, and the other oxygen atom of NO_2 will be denoted O_N.

Adsorption of NO_2 on the surfaces results in significant elongation of the N−O_V bond length from its gas-phase value of 1.21 Å to 1.36 Å on the (111) surface, 1.31 Å on the (110) surface, and 1.44 Å on the (100) surface. The N−O_N distance changes only slightly, being 1.23, 1.25, and 1.19 Å on the (111), (110), and (100) surfaces, respectively. Although there is significant lengthening of the N−O_V bond, it is clear that dissociation to NO and oxygen is not observed, indicating that there is an energy barrier to the breaking of this bond. Experimental data suggests that a temperature from around 300 (for reduced ceria[4]) to 400 K (with Pt present[2]) is needed for NO_2 dissociation.

In analyzing changes in the surface atomic structure upon adsorption of NO_2, we focus on the local structure around the Ce(III) ions of the defective surface. Table 1 presents the Ce−O distances for Ce^A (yellow sphere) and Ce^B (orange sphere) in the stoichiometric, bare reduced surfaces and reduced surfaces with NO_2 adsorbed, which involve the Ce(III) ions that are formed upon reduction of the surface.

In the stoichiometric (111) surface (in which there are no Ce(III) ions), each surface Ce is coordinated to three surface oxygen atoms, with identical Ce−O distances of 2.36 Å. In the reduced surface, two Ce(III) ions are formed; the Ce−O distances involving the Ce(III) ions are 2.37 Å, with the lengthening due to formation of the Ce(III) ions, which have a reduced Coulombic interaction with neighboring oxygen atoms. When NO_2 adsorbs onto the surface, O_V is closer to Ce^B, with a Ce−O_V distance of 2.66 Å, compared to Ce^A, which shows a Ce−O_V distance of 2.80 Å. Both of these distances are significantly longer than Ce(IV)−O distances. In the surface itself, the two Ce(III) ions behave differently. Ce^A shows Ce−O distances that are elongated by 0.05 Å, while for Ce^B, the distances have contracted to 2.30/2.32 Å (0.05/0.07 Å contraction).

In the stoichiometric (110) surface, with no Ce(III) ions, the surface Ce−O distances are 2.33 Å. Upon formation of the reduced bare surface, two Ce(III) ions are formed, with a single oxygen atom, O^{Br}, bridging them so that these Ce atoms are coordinated to three surface oxygen atoms; the Ce(III)−O^{Br} distances show an elongation of 0.07 Å, with two remaining pairs of Ce−O distances (2.27 and 2.32 Å). When NO_2 is adsorbed onto the reduced surface, O_V is again found to be closer to Ce^B than Ce^A, with Ce−O distances of 2.60 and 2.77 Å, respectively. In the surface, the Ce^A to bridging oxygen distance is elongated by 0.03 Å, while that involving Ce^B is shortened by 0.16 Å (Ce^B). The remaining surface Ce−O distances are 2.35/2.36 Å (Ce^A) and 2.19/2.21 Å (Ce^B), indicating substantially shorter Ce−O distances involving Ce^B, compared to Ce^A.

In the stoichiometric (100) surface, the surface oxygen atoms are two coordinate and the surface Ce−O distances are 2.19 Å. In the reduced surfaces, there is a lengthening of 0.04 Å in the row containing the vacancy, again due to the presence of Ce(III) ions. Upon adsorption of NO_2, the Ce−O_V distances are again shorter for Ce^B (2.43 Å) than for Ce^A (2.50 Å). In the surface, the Ce^A−O distance undergoes an elongation 0.08 Å compared to the reduced surface, while the Ce^B−O distance is shortened by 0.19 Å.

We observe structural modifications upon formation of the reduced surface and subsequent adsorption of NO_2 that are similar for all surfaces. Formation of the reduced surface produces 2 Ce(III) ions, which show elongated Ce−O distances, due to the presence of the Ce(III) ion. When the molecule interacts with the reduced surface we find the following: (i) the O_V atom is found closer to one of the Ce(III) ions of the reduced surface (Ce^B) than the other, (ii) the Ce(III)−O distances in the reduced surface are strongly modified, with elongation of Ce^A−O and shortening of Ce^B−O distances, and (iii) the N−O_N bond points toward Ce^B, which has the shorter Ce−O_V distance.

3.2. Electronic Structure of NO_2 Adsorbed onto Ceria Surfaces. The electronic structure of stoichiometric ceria is well-known.[6,7,9−11] The valence band is derived from O 2p states, a narrow unoccupied Ce 4f band lies about 3.0 eV above the valence band, and the Ce 5d-derived conduction band lies 5.0 eV above the valence band. When a ceria surface is reduced, UPS shows the presence of a gap state between the valence band and the unoccupied Ce 4f states; this gap state has been shown to be derived from partial occupation of Ce 4f states,[16] which has also been seen with DFT+U calculations.[10,11,15] Gas-phase NO_2 is a radical, with one unpaired electron found in the highest occupied MO (HOMO).

The general features of the electronic densities of states (EDOS) for NO_2 adsorption are similar for all three surfaces, and we will only display the total EDOS and the ionic and angular momentum decomposed partial EDOS, PEDOS, for the example of the (111)-NO_2 surface−adsorbate structure. We focus on modifications to the surface and the molecular PEDOS as a result of the interaction, allowing a determination of the nature of any charge transfer from the surface to the molecule.

In the total EDOS of Figure 2 (the top of the valence band is set to the zero of the energy scale) we find the following ceria-derived peaks: (i) a wide band below −12 eV (Ce 5p-derived), (ii) a wide band stretching from 0 to −4.5 eV

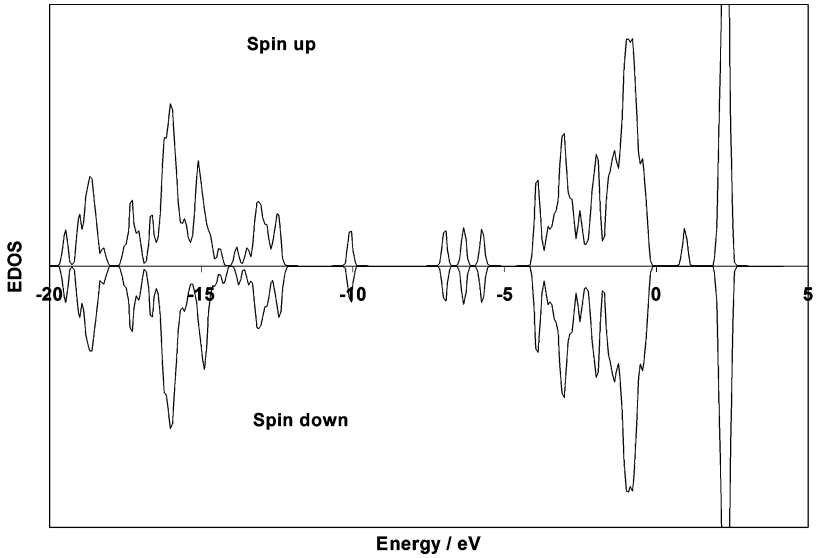

Figure 2. Total EDOS for (111)-NO_2 from DFT+U.

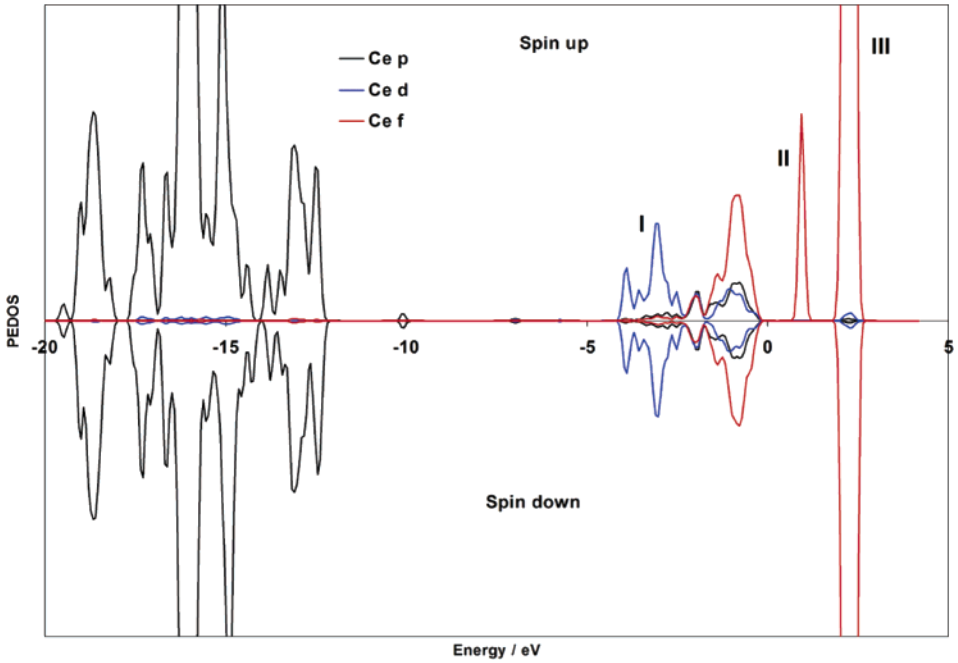

Figure 3. Ce PEDOS for (111)-NO_2 from DFT+U.

(the O 2p valence band), and (iii) the narrow unoccupied Ce 4f band lying above the valence band. In addition, there is a small narrow peak lying between the top of the valence band and the bottom of the unoccupied Ce 4f-derived peak, which is due to the presence of reduced ceria and is a signature of the presence of reduced Ce(III) ions in theoretical and experimental studies of reduced ceria.[10,11,15,16] Between the Ce 5p band and the valence band, we find some narrow EDOS peaks which are not present in the EDOS of pure or reduced ceria.[10,15]

We present in Figure 3 the PEDOS for the Ce ions of (111)-NO_2. The PEDOS is similar to that for reduced ceria, in particular the presence of the Ce 4f-derived gap state (region II in Figure 3) lying between the valence band (region I) and the empty Ce 4f band (region III).[10,11,15] The offset from the valence band to the gap state is 1.05 eV for the (111) surface, 1.05 eV for the (110) surface, and 0.80 eV for the (100), all of which are little modified compared to those of the reduced surfaces.[10,15] This analysis confirms that reduced Ce(III) ions are still present upon adsorption of NO_2 on a reduced ceria surface.

The nature of the adsorbed NO_2 species is established through analysis of the N 2p and O 2p PEDOS for the adsorbate (Figure 4 a), gas-phase neutral NO_2 (Figure 4b), and the gas-phase NO_2^- anion (Figure 4c). The PEDOS for neutral NO_2 shows an open shell character, while for the adsorbed species, we find spin pairing of the N and O 2p bands. A similar spin pairing is present for the NO_2^- anion. The neutral NO_2 and adsorbed NO_2 PEDOS are inconsistent, demonstrating that the adsorbed species cannot be neutral NO_2.

The nature of the highest occupied molecular orbital (HOMO, marked "H" in Figure 4, parts a and c) and the LUMO (marked "L") is the same for the adsorbate and the NO_2^- anion; the HOMO is predominantly O 2p-derived, with N 2p character, while the LUMO is derived from equal O 2p and N 2p contributions. The HOMO−LUMO gap in both cases is also very similar. On the other hand for neutral NO_2, while the nature of the HOMO is the same as NO_2^- and adsorbed NO_2, we see in Figure 4, that the nature of the LUMO of neutral NO_2 is different with a considerably smaller HOMO−

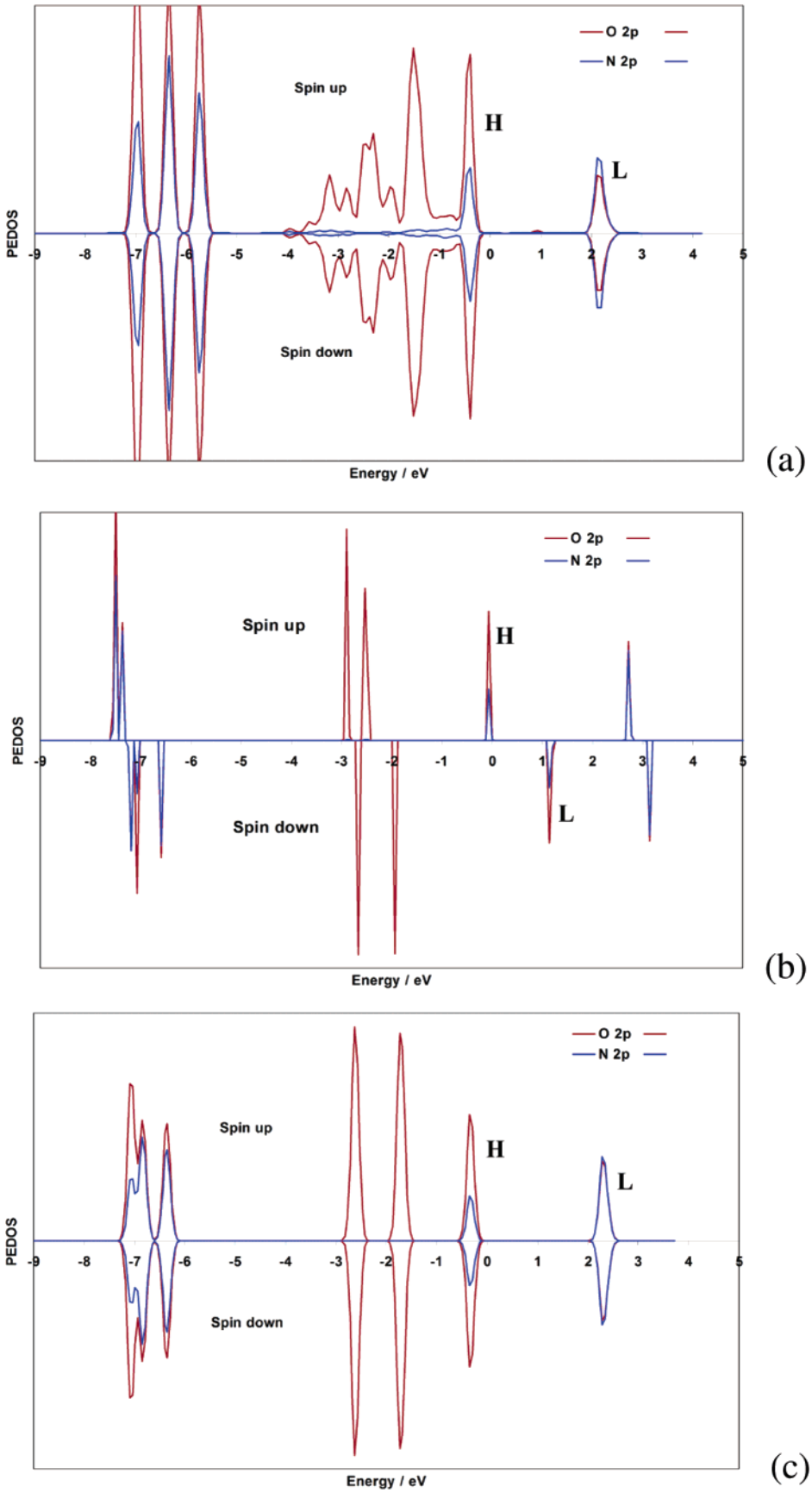

Figure 4. (a) N and O 2p PEDOS for adsorbed NO_2, (b) N and O 2p PEDOS for gas-phase NO_2, and (c) N and O 2p PEDOS for gas-phase NO_2^-.

LUMO gap. The additional O 2p states centered around 2.50 eV below the HOMO for adsorbed NO_2, which are not present for gas-phase NO_2^-, are due to the presence of the oxide surface. From this analysis of the electronic structure, it is clear that the adsorbed species is an NO_2^- anion.

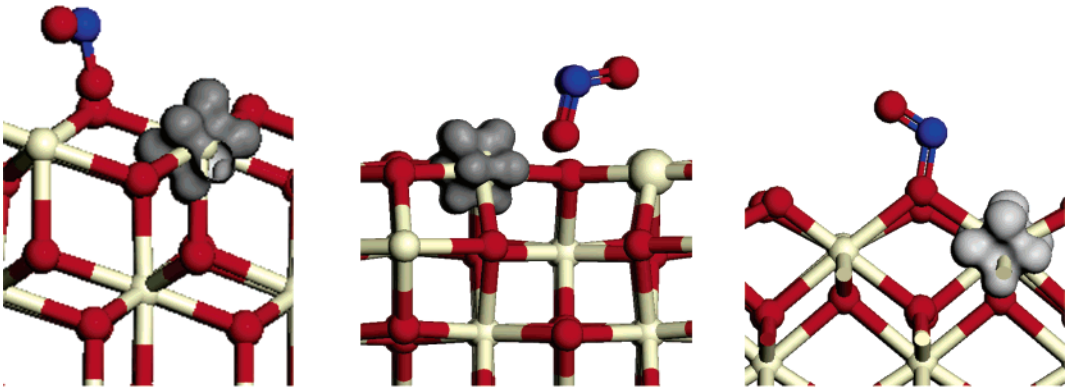

Figure 5. Isosurface plot for the spin density for (a) the (111) surface, (b) the (110) surface, and (c) the (100) surface from DFT+U.

Partial atomic charges, derived from projection of the wave function onto spherical harmonics, show that the total charge on adsorbed NO_2 has increased by 0.80 electrons. In addition, the observed lengthening of the $N-O_V$ bond upon adsorption further supports the presence of an anionic NO_2^- species. Symmetric elongation of the N−O bond distances from 1.21 to 1.26 Å is seen in gas-phase NO_2^-, with the asymmetric bond elongation found in the adsorbed species due to the asymmetric electric field present at the surface as well as activation of the molecule toward N−O bond cleavage.

The excess spin density resulting from a full spin relaxation is plotted in Figure 5 for the three surfaces. The spin density shows the presence of excess spin on a *single* reduced Ce(III) ion (Ce^A) neighboring the vacancy site for all surfaces. In the reduced surface, there are two Ce(III) ions neighboring the vacancy site. Thus, we see from the electronic structure, that upon adsorption of NO_2, one Ce(III) ion is reoxidized to Ce(IV), with an electron transferred from the surface to NO_2, forming NO_2^-. Note also that the shape of the isosurface is that of an f orbital, which we expect since a Ce(III) ion has a $4f^1$ electronic configuration.

The conclusions regarding the nature of the surface Ce ions derived from the electronic structure above can be further supported by returning to the geometry analysis. Ce^A has been shown to display elongated Ce−O distances, characteristic of a reduced Ce(III) ion, and furthermore, this is the Ce ion on which the spin density in Figure 5 is found. The presence of this reduced Ce ion leads to the Ce 4f-derived gap state found in the electronic density of states of Figures 2 and 3. Ce^B displays Ce−O distances characteristic of a Ce(IV) ion, and the spin density shows clearly that this Ce is indeed reoxidized to Ce(IV), with transfer of an electron to adsorbed NO_2. These conclusions show no surface sensitivity leading us to conclude that upon adsorption of NO_2 on a reduced ceria surface, there is reoxidation of one of the Ce(III) ions to Ce(IV) and a partial reduction of the adsorbed NO_2 molecule to NO_2^-.

3.3. Energetics of NO_2 Adsorption on Defective Ceria Surfaces. Finally, we consider the energetics for the adsorption of NO_2 on each surface:

$$CeO_{2-x} + NO_2 \rightarrow [NO_2]^-[CeO_{2-x}]^+$$

where $[NO_2]^-[CeO_{2-x}]^+$ is the surface−adsorbate structure, in which an electron has been transferred from reduced ceria to the NO_2 molecule so that the surface is partially reoxidized. For computation of the total energies, stoichiometric ceria (CeO_2), reduced ceria (CeO_{2-x}), and the surface-molecule structure ($[NO_2]^-[CeO_{2-x}]^+$) are described with DFT+U (since there are Ce f states present in these structures).[15,19]

The adsorption energy is negative, showing that formation of the surface−adsorbate complex is favorable, and the adsorption energies are −2.40 eV for the (111) surface, −2.25 eV for the (110) surface, and −2.32 eV for the (100) surface. Energy gains of this magnitude along with the geometrical and electronic data given above confirm the strong interaction between the molecule and the oxide surface.

For the reaction in which NO_2 is reduced to NO and the defective ceria surface is fully reoxidized

$$CeO_{2-x} + NO_2 \rightarrow CeO_2 + NO$$

the reaction energies are also exothermic with values of −1.52 eV for the (111) surface, −0.93 eV for the (110) surface, and −1.20 eV for the (100) surface. We can rationalize these energies in the following fashion. Since the stoichiometric surface is being reformed, it may be expected that the reaction energies should follow the stability given by the surface energies ((111) < (110) < (100)). Hence, the more stable (111) surface would be expected to have the most exothermic reaction energy. Although this is indeed the case, the order for the (110) and (100) surfaces is reversed. We instead rationalize this finding using the vacancy formation energies, for which (110) < (100) < (111).[15] This is the same as the ordering of the reaction energies. Thus, for the present case, the generation of the reoxidized surface through interaction with NO_2 is most favorable on the (111) surface, since an oxygen vacancy is least stable on this surface. Conversely, the (110) surface is most favored for vacancy formation so that it is the least favorable surface for NO_2 dissociation. Comparison of the reaction energies with the adsorption energies shows that an energy cost of around 1.0 eV is needed to remove NO after adsorption of NO_2, which is consistent with the temperatures needed for the reaction to occur in.[2,4]

4. Conclusions

The present paper is a first-principles examination of the surface structure and electronic structure of NO_2 adsorbed onto defective low-index (111), (110), and (100) surfaces of ceria with the aim of contributing to the understanding of the process of the conversion of NO_2 to NO over reduced ceria. Such a study provides a detailed understanding of the atomic level details involved in the reaction of NO_2 with defective ceria surfaces and helps to rationalize the results obtained for the energetics of NO_2 to NO conversion.

Our results show that upon adsorption of NO_2 onto defective ceria surfaces, some reoxidation of the Ce^{3+} ions takes place, with an electron being transferred from the surface to the NO_2 molecule, to form NO_2^- as an intermediate adsorption structure. Lengthening of one N−O bond by around 10% is found, which is a necessary step in the formation of free NO and full reoxidation of the surface. Evidence for this process comes from the surface and electronic structure upon adsorption, both of which demonstrate the reoxidation of one of the two Ce^{3+} ions found in defective ceria surfaces. An analysis of the electronic density of states and charge partitioning shows the presence of an NO_2^- species which forms due to charge transfer from the surface to the molecule.

The adsorption energies show an energy gain of at least 2.25 eV, while the energetics for the conversion of NO_2 to NO show that this process is most favorable on the (111) surface. Although the overall reaction for conversion of NO_2 to NO is exothermic, there is an energy cost involved in the decomposition of adsorbed NO_2^-.

Acknowledgment. We acknowledge support for this work from the Petroleum Research Fund administered by the American Chemical Society, Science Foundation Ireland (Grant 04/BR/C0216) and the EPSRC (Grants GR/S48431/1, GR/S48448/01). We also acknowledge the EPSRC for funding of and access to the Mott2 computer, under Grant GR/S84415/01.

References and Notes

(1) Trovarelli, A. *Catalysis by Ceria and Related Materials*; Imperial College Press: London, U.K., 2002.

(2) Berner, U.; Schierbaum, K.; Jones, G.; Wincott, P.; Haq, S.; Thornton, G. *Surf. Sci.* **2000**, *467*, 201.

(3) Mullins, D. R.; Overbury, S. H. *Surf. Sci.* **2002**, *511*, L293.

(4) Rodriguez, J. A.; Jirsak, T.; Sambasivan, S.; Fischer, D.; Maiti, A. *J. Chem. Phys.* **2000**, *112*, 9929.

(5) Namai, Y.; Fukui, K.; Iwasawa, Y. *Nanotechnology* **2004**, *15*, S49.

(6) Hill, S. E.; Catlow, C. R. A. *J. Phys. Chem. Solids* **1993**, *54*, 411.

(7) Skorodumova, N. V.; Ahuja, R.; Simak, S. I.; Abrikosov, I. A.; Johansson, B.; Lundqvist, B. I. *Phys. Rev. B* **2001**, *64*, 115108.

(8) Gennard, S.; Cora, F.; Catlow, C. R. A. *J. Phys. Chem. B* **1999**, *103*, 10158.

(9) Skorodumova, N. V.; Baudin, M.; Hermansson, K. *Phys. Rev. B* **2004**, *69*, 075401.

(10) Nolan, M.; Grigoleit, S.; Sayle, D. C.; Parker, S. C.; Watson, G. W. *Surf. Sci.* **2005**, *576*, 217.

(11) Fabris, S.; de Gironcoli, S.; Baroni, S.; Vicario, G.; Balducci, G. *Phys. Rev. B* **2005**, *71*, 041102.

(12) Sayle, T. X. T.; Parker, S. C.; Catlow, C. R. A. *Chem. Commun.* **1992**, 977.

(13) Conesa, J. C. *Surf. Sci.* **1995**, *339*, 337.

(14) Yang, X. Z.; Woo, T. K.; Baudin, M.; Hermansson, K. *J. Chem. Phys.* **2004**, *120*, 7741.

(15) Nolan, M.; Parker, S. C.; Watson, G. W. *Surf. Sci.* **2005**, *595*, 223.

(16) Henderson, M. A.; Perkins, C. L.; Engelhard, M. H.; Thevuthasan, S.; Peden, C. H. F. *Surf. Sci.* **2003**, *526*, 1.

(17) (a) Anisimov, V. I.; Zaanen, J.; Andersen, O. K. *Phys. Rev B* **1991**, *44*, 943. (b) Dudarev, S. L.; Botton, G. A.; Savrasov, S. Y.; Humphreys C. J.; Sutton, A. P. *Phys. Rev. B* **1998**, *57*, 1505.

(18) Shick, A. B.; Pickett, W. E.; Liechtenstein, A. I. *J. Electron. Spectrosc.* **2001**, *114*, 753.

(19) Nolan, M.; Watson, G. W. *Surf. Sci.* **2005**, *586*, 25.

(20) (a) Kresse, G.; Hafner, J. *Phys. Rev. B* **1994**, *49*, 14251. (b) Kresse, G.; Furthmüller, J. *Phys. Rev. B* **1996**, *54*, 11169.

(21) (a) Blöchl, P. E. *Phys. Rev. B* **1994**, *50*, 17953. (b) Kresse, G.; Joubert, D. *Phys. Rev. B* **1999**, *59*, 1758.

(22) Perdew, J. P. In *Electronic Structure of Solids '91*; Ziesche, P., Eschrig, H., Eds.; Akademie Verlag: Berlin, 1991.